PM73kB

# A NOVEL ATTITUDE DETERMINATION ALGORITHM FOR SPINNING SPACECRAFT

Itzhack Y. Bar-Itzhack[#]
*Technion-Israel Institute of Technology, Haifa, Israel, 32000*

and

Richard R. Harman[¶]
*NASA Goddard Space Flight Center, Greenbelt, MD, 20771*

## Abstract

This paper presents a single frame algorithm for the spin-axis orientation-determination of spinning spacecraft that encounters no ambiguity problems, as well as a simple Kalman filer for continuously estimating the full attitude of a spinning spacecraft. The later algorithm is comprised of two low order decoupled Kalman filters; one estimates the spin axis orientation, and the other estimates the spin rate and the spin (phase) angle. The filters are ambiguity free and do not rely on the spacecraft dynamics. They were successfully tested using data obtained from one of the ST5 satellites.

## I. Introduction

In the early days of space exploration, the use of spinning satellites was prevalent for spacecraft (SC) stabilization [Reference 1, Chapters 10, 11]. In that era only batch algorithms were used in order to determine the attitude of the spinning satellites. Starting in the late 1970s, the focus has shifted from spinning satellites to three-axis stabilized SC [Reference 1, Chapter 12]. Considerable effort was invested in devising accurate algorithms for attitude determination (AD). In particular, a variety of recursive AD algorithms were introduced. As a result, spinning SC development and their resulting ground system development stagnated. In the 1990s, shrinking budgets made spinning SC an attractive option for science. The attitude

[#] Professor Emeritus, Faculty of Aerospace Engineering, Member Asher Space Research Institute ibaritz@technion.ac.il, + 972-4-829-3196, AIAA Fellow, IEEE Fellow.

[¶] Aerospace Engineer, Flight Dynamics Analysis Branch, Code 595, richard.r.harman@nasa.gov, 301-286-5125.

requirements for recent spinning SC are more stringent and the ground systems must be enhanced in order to provide the necessary attitude estimation accuracy, and yet suitable recursive algorithms for spinning SC did not exist. Therefore when the use of spinning SC re-emerged, efforts were made to develop such algorithms. Baker[2], for example, developed a Kalman filter (KF) based on a dynamic model presented by Markley, Seidewitz and Nicholson[3]. The attitude was represented by Euler angles. The first derivatives of the states were nonlinear (trigonometric) functions of the states themselves. Simplifying assumptions had to be adopted in order to use the dynamics model in an extended KF. Sedlak[4] used Markley Variables[5] to describe the SC attitude dynamics. These variables are slowly varying which facilitates the filter state tracking and estimation, but the models which have to be used in the KF are quite complicated. Bar-Itzhack and Harman used a pseudo linear filter[6] to do the same[7]. The philosophy that governed the newly developed recursive filters for AD of spinning SC was an extension of the concepts on which three-axis stabilized AD algorithms were founded. Accordingly, other than [7], there was no separation between the spin axis orientation states and the spin angle states. Thus, the slowly changing dynamics of the spin axis orientation was combined into one dynamics model that included the fast changing spin (phase) angle.

The present algorithm is based on the premise that the parameters which describe the direction of the spin axis orientation in inertial space vary slowly even when the SC nutates and precesses. The spin (phase) angle, on the other hand, changes fast but stays almost at a constant rate per a single revolution and is decoupled from the other axes. In fact, this is the classical approach to spin-axis orientation determination (ORD) [Reference 1, Chapters, 10, 11]. (A good exposition of the difference in approach to three-axis AD and spin-axis ORD is presented in Reference 8.) This realization enables the decoupling of the recursive AD algorithm into two simple low-order filters that are independent of the SC dynamics.

There are two approaches to spin-axis ORD. One relies heavily on the solution of trigonometric functions [Reference 1, Chapters 10, 11]. The other approach is a vectored approach[9, 8]. This is the approach adopted in the present work; however, unlike in References 8 and 9, here we develop two recursive algorithms, one for obtaining a single frame solution and the other is a novel Kalman filter for time varying ORD which is based on multiple measurements performed at different time points. Also, here the components of the spin axis are found as projections on the axes of the Geocentric Inertial Coordinates (GCI) rather than projections on the measured directions and their cross product, as presented in Eq. (1) of [9], Eq. (11-3e) of [1], and Eq. (2) of [8]. In the present work we are not concerned with the measurement techniques. This topic can be found in other works [see e.g. References 1 and 10].

As is well known, when only two vector measurements are available for spin axis ORD, there exist two possible solutions [see e.g. Reference 1, Chapters 10, 11 and Reference 8]. The cause of this ambiguity is explained and a solution is proposed, which does not rely on cumbersome spherical geometry solutions.

In the following section we discuss the geometry of the ORD problem. The ambiguity problem generated by the existence of two possible solutions is explained in Section III whereas in Section IV we present a simple vector solution to the ambiguity problem. Section V presents a simple low order Kalman filter (KF) for the spin axis ORD, and an even simpler one for estimating the spin (phase) angle. Results are presented in Section VI, a discussion of these results is given in Section VII, and the conclusions from this work are presented in the last section.

## II. Connections between the Spin Axis Orientation and Vector Measurements

Consider Fig. 1 where the sun sensor measurement is expressed by the components of the unit vector in the sun direction, resolved in the GCI coordinate system. These components are $s_{Ix}$, $s_{Iy}$ and $s_{Iz}$. Similarly, the *normalized* three-axis magnetometer (TAM) measurement is expressed by the three components, $m_{Ix}$, $m_{Iy}$ and $m_{Iz}$ (the TAM vector, $\mathbf{m}$, is shown in the figure but its components are not shown). We want to find the direction of $\mathbf{Z}_b$ in the GCI coordinates expressed by its components along the coordinate axes. When we know these components, we can certainly express the direction of $\mathbf{Z}_b$ by the angles $\alpha$ and $\beta$, if required. Denote the components of $\mathbf{Z}_b$ in the inertial coordinates, GCI, by x, y and z. In the filter that will be presented later, we estimate $\mathbf{Z}_b$ where $\mathbf{Z}_b^T = [x \quad y \quad z]$.

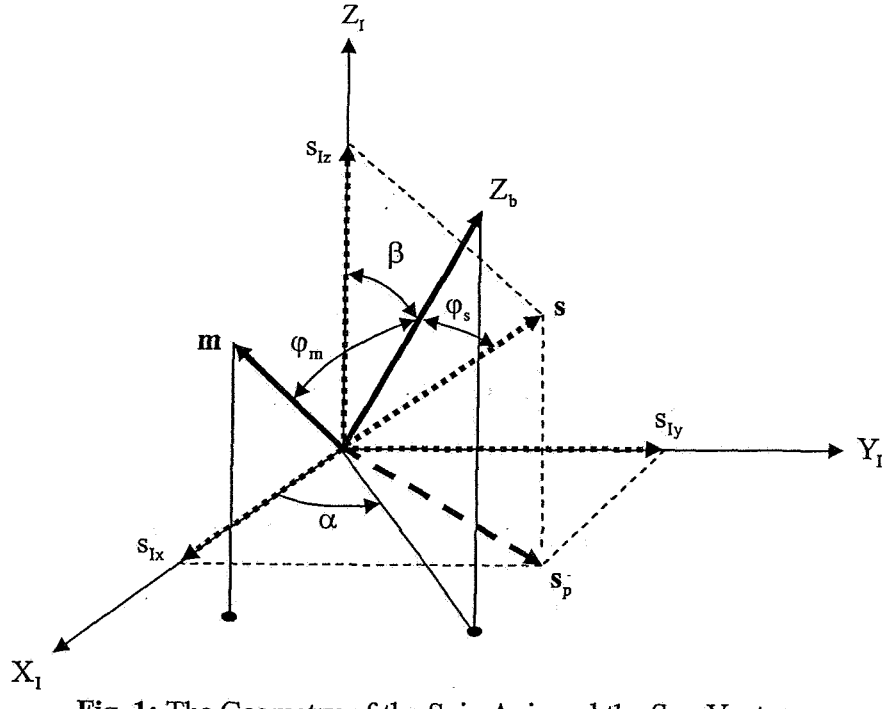


**Fig. 1:** The Geometry of the Spin Axis and the Sun Vector

Since the sun angle, $\varphi_s$, is measured, we can calculate its cosine. Let us denote this

cosine by $U_s$; that is

$$U_s = \cos\varphi_s \tag{1}$$

We note that the cosine of $\varphi_s$, which is the angle between the sun vector and $\mathbf{Z}_b$, is nothing but $s_{bz}$. On the other hand the cosine of $\varphi_s$ is equal to the dot product of $\mathbf{Z}_b$ and $\mathbf{s}$; hence we can write

$$U_s = s_{Ix}x + s_{Iy}y + s_{Iz}z \tag{2}$$

Like with the sun sensor measurement, the cosine of the angle between the normalized TAM-vector and $\mathbf{Z}_b$ is simply $m_{bz}$ (see Fig. 2); that is,

$$\cos\varphi_m = m_{bz} \tag{3}$$

Denote this cosine by $U_m$

$$U_m = \cos\varphi_m \tag{4}$$

Like with the sun sensor, we know that $\mathbf{Z}_b \cdot \mathbf{m} = \cos\varphi_m$, hence

$$U_m = m_{Ix}x + m_{Iy}y + m_{Iz}z \tag{5}$$

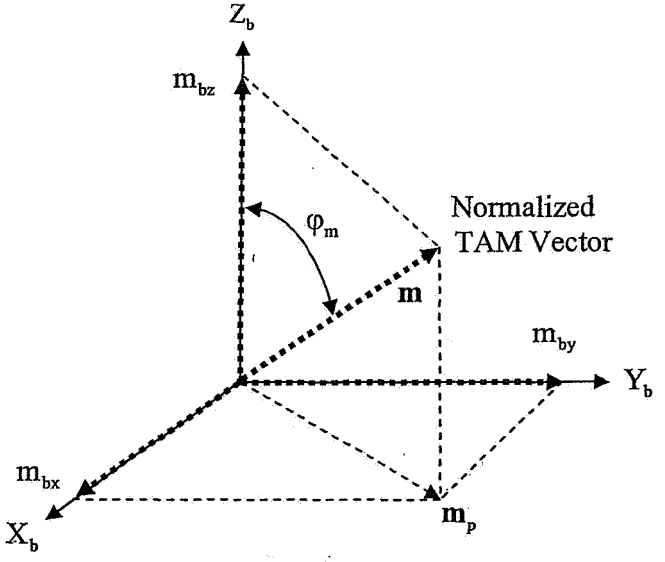


**Fig 2:** The Illustration of $\varphi_m$

Combining Eqs. (2) and (5) into one matrix equation yields

$$\begin{bmatrix} U_s \\ U_m \end{bmatrix} = \begin{bmatrix} s_{Ix} & s_{Iy} & s_{Iz} \\ m_{Ix} & m_{Iy} & m_{Iz} \end{bmatrix} \begin{bmatrix} x \\ y \\ z \end{bmatrix} \tag{6}$$

## III. The Ambiguity Problem

Equation (6) can be satisfied by two solutions. This is because, as is well known[9,1,8], the spin axis can lie along two different lines. As shown in Fig. 3, these lines are formed by the intersection of two cones; namely, the sun cone and the magnetic field cone. These cones are described as follows. The main axis of the sun cone is the sun line, **s**, and the main axis of the magnetic field cone coincides with the normalized magnetic field vector, **m**.

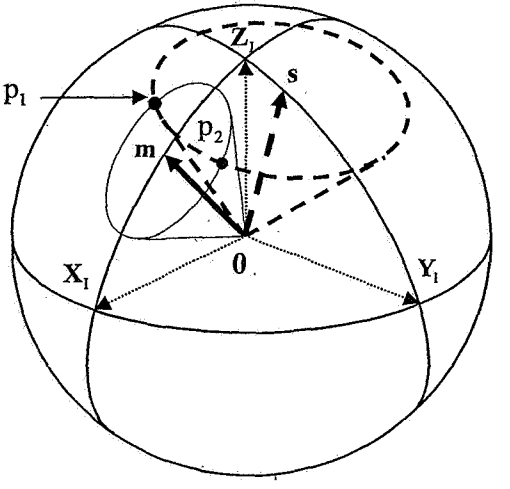


**Fig. 3:** The Geometry that Depicts the Two Possible Solutions.

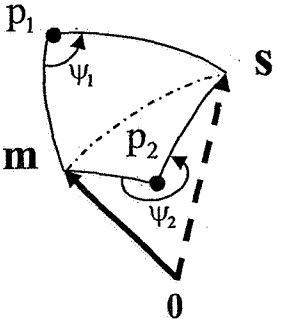


**Fig. 4:** Upper View of the Two Possible Solutions.

The sun cone is generated by a rotation about the sun direction of a line that forms the cone half-angle $\varphi_s$ with the sun line. Similarly, the magnetic field cone is formed by a rotation about the magnetic field line of a line that forms the cone half-angle $\varphi_m$ with the magnetic field line. The two possible solutions are the line from **0** to $p_1$ and the line from **0** to $p_2$ (the lines themselves are not shown in the figure). An upper look at points $p_1$, $p_2$, s and m is presented in Fig. 4. The existence of two possible solutions can be demonstrated through the following example.

Suppose that $\mathbf{Z}_{bI}$, the spin axis unit vector expressed in the GCI coordinates, is as follows

$$\mathbf{Z}_{bI} = \begin{bmatrix} 0.612 \\ 0.354 \\ 0.707 \end{bmatrix} \tag{13.a}$$

Also suppose that

$$\mathbf{s}_I = \begin{bmatrix} -0.176 \\ 0.44 \\ 0.88 \end{bmatrix} \tag{13.b}$$

$$\mathbf{m}_I = \begin{bmatrix} 0.162 \\ -0.566 \\ 0.808 \end{bmatrix} \tag{13.c}$$

where $\mathbf{s}_I$ and $\mathbf{m}_I$ are, respectively, a unit vector in the sun direction, and a unit vector in the direction of the magnetic field, both expressed in the GCI coordinates. Then the matrix $H$, which is embedded in Eq. (6), and is defined as

$$H = \begin{bmatrix} s_{Ix} & s_{Iy} & s_{Iz} \\ m_{Ix} & m_{Iy} & m_{Iz} \end{bmatrix} \tag{13.d}$$

takes the value

$$H = \begin{bmatrix} -0.176 & 0.44 & 0.88 \\ 0.162 & -0.566 & 0.808 \end{bmatrix} \tag{13.e}$$

In this case $U_s \triangleq \mathbf{Z}_b \cdot \mathbf{s}_I = 0.67$ and $U_m \triangleq \mathbf{Z}_b \cdot \mathbf{m}_I = 0.471$. The following two solutions $\mathbf{Z}_{bI1} = [-0.743 \quad -0.098 \quad 0.662]$ and $\mathbf{Z}_{bI2} = [0.612 \quad 0.354 \quad 0.707]$ satisfy Eq. (6). Indeed, Eq. (6) takes the following two correct forms

$$\begin{bmatrix} 0.67 \\ 0.471 \end{bmatrix} = \begin{bmatrix} -0.176 & 0.44 & 0.88 \\ 0.162 & -0.566 & 0.808 \end{bmatrix} \begin{bmatrix} -0.743 \\ -0.098 \\ 0.662 \end{bmatrix} \tag{13.f}$$

and

$$\begin{bmatrix} 0.67 \\ 0.471 \end{bmatrix} = \begin{bmatrix} -0.176 & 0.44 & 0.88 \\ 0.162 & -0.566 & 0.808 \end{bmatrix} \begin{bmatrix} 0.612 \\ 0.354 \\ 0.707 \end{bmatrix} \tag{13.g}$$

A way to resolve the ambiguity problem is presented next.

## IV. Ambiguity Resolution

While other ways to solve the ambiguity problem also exist [see e.g. Ref. 8], we chose a rather simple approach to resolve the ambiguity problem, and indeed to solve for $\mathbf{Z}_{bI}$, which avoids tedious spherical geometry calculations. Our solution to the problem is as follows.

Let $\mathbf{s}_I$ and $\mathbf{m}_I$ be, respectively, unit vectors in the direction of the sun and the magnetic field resolved in the GCI system. Similarly let $\mathbf{s}_b$ and $\mathbf{m}_b$ be the same in the body system. Let the transformation matrix from the body to the GCI coordinate system be denoted by $D_I^b$, then obviously

$$\left[ \mathbf{s}_I \mid \mathbf{m}_I \mid \mathbf{s}_I \times \mathbf{m}_I \right] = D_I^b \left[ \mathbf{s}_b \mid \mathbf{m}_b \mid \mathbf{s}_b \times \mathbf{m}_b \right] \tag{14.a}$$

let

$$C = \left[ \mathbf{s}_I \mid \mathbf{m}_I \mid \mathbf{s}_I \times \mathbf{m}_I \right] \quad (14.b) \qquad B = \left[ \mathbf{s}_b \mid \mathbf{m}_b \mid \mathbf{s}_b \times \mathbf{m}_b \right] \quad (14.c)$$

then

$$D_I^b = CB^{-1} \tag{14.d}$$

Now $\mathbf{Z}_{bb}$, which is $\mathbf{Z}_b$, resolved in body coordinates, is given by $\mathbf{Z}_{bb}{}^T = [0 \quad 0 \quad 1]$, and since

$$\mathbf{Z}_{bI} = D_I^b \mathbf{Z}_{bb} \tag{14.e}$$

then

$$\mathbf{Z}_{bI} = \mathbf{d}_{I3}^b \tag{14.f}$$

where $\mathbf{d}_{I3}^{b}$ is the third column of $D_I^b$. Note that the two vector measurements have to be taken at certain time points; namely, at times when the sun sensor acquires the sun.

The method proposed here is demonstrated through the following example. Let $\mathbf{Z}_{bI}$, $\mathbf{s}_I$ and $\mathbf{m}_I$ be as before. Suppose that the SC is oriented such that

$$\mathbf{s}_b = \begin{bmatrix} 0.227 \\ -0.706 \\ 0.67 \end{bmatrix} \quad (15.a) \qquad \text{and} \qquad \mathbf{m}_b = \begin{bmatrix} 0.875 \\ 0.113 \\ 0.471 \end{bmatrix} \quad (15.b)$$

where $\mathbf{s}_b$ is $\mathbf{s}$ resolved in the body coordinates and $\mathbf{m}_b$ is the $\mathbf{m}$ vector also resolved in the body frame. Computing the $C$, $B$, and $D_I^b$ matrices defined, respectively, in Eqs. (14.b, c and d) yields

$$C = \begin{bmatrix} -0.176 & 0.162 & 0.854 \\ 0.44 & -0.566 & 0.285 \\ 0.88 & 0.808 & 0.028 \end{bmatrix} \quad (15.c) \qquad B = \begin{bmatrix} 0.227 & 0.875 & -0.408 \\ -0.706 & 0.113 & 0.48 \\ 0.67 & 0.471 & 0.644 \end{bmatrix} \quad (15.d)$$

$$D_I^b = \begin{bmatrix} -0.242 & 0.753 & 0.612 \\ -0.768 & -0.534 & 0.354 \\ 0.593 & -0.385 & 0.707 \end{bmatrix} \quad (15.e)$$

It is seen that the third column of $D_I^b$ is $\mathbf{Z}_{bI}$ given in Eq. (13.a) which is $\mathbf{Z}_{bI2}$, the second of the two solutions, found before, of Eq. (6). It should be noted that $D_I^b$ can be found using the TRIAD algorithm[11,12] where unlike in Eq. (14.d), there is no need to invert a matrix. We chose to use the present method for computing $D_I^b$ because TRIAD is a more elaborate routine whereas, being a $3 \times 3$ matrix, the inverse of $B$ can be computed analytically.

## V. A Novel Kalman Filter for Determination of the Attitude

The filter that is presented here consists of two linear reduced-order filters. The first filter estimates the spin axis orientation, $\mathbf{Z}_{bI}$, whereas the second filter estimates the spin

(phase) angle. Once the initial estimate of $\mathbf{Z}_{bf}$ is close to its correct value, the filter recursively produces a better estimate of it. The purpose of the discussion of the ambiguity and its resolution presented in the preceding sections was aimed at supplying the correct initial estimate, free of ambiguity.

**V.1 A simple Low-Order KF for spin axis determination**

Recall Eq. (6)

$$\begin{bmatrix} U_s \\ U_m \end{bmatrix} = \begin{bmatrix} s_{Ix} & s_{Iy} & s_{Iz} \\ m_{Ix} & m_{Iy} & m_{Iz} \end{bmatrix} \begin{bmatrix} x \\ y \\ z \end{bmatrix} \tag{6}$$

Since $U_s$ and $U_m$ are the result of measurements, we add to the last equation some appropriate zero-mean white-noise components $v_s$ and $v_m$, and obtain the measurement equation

$$\begin{bmatrix} U_s \\ U_m \end{bmatrix} = \begin{bmatrix} s_{Ix} & s_{Iy} & s_{Iz} \\ m_{Ix} & m_{Iy} & m_{Iz} \end{bmatrix} \begin{bmatrix} x \\ y \\ z \end{bmatrix} + \begin{bmatrix} v_s \\ v_m \end{bmatrix} \tag{16.a}$$

Since between measurements the direction of the spin axis of a spin stabilized SC does not change much, it is appropriate to model the dynamics of its components between measurements as a Markov process[13]. That is

$$\begin{bmatrix} \dot{x} \\ \dot{y} \\ \dot{z} \end{bmatrix} = \begin{bmatrix} -1/\tau_x & 0 & 0 \\ 0 & -1/\tau_y & 0 \\ 0 & 0 & -1/\tau_z \end{bmatrix} \begin{bmatrix} x \\ y \\ z \end{bmatrix} + \begin{bmatrix} w_x \\ w_y \\ w_z \end{bmatrix} \tag{16.b}$$

Eqs. (16) constitute a measurement model and a dynamics model which are suitable for a simple linear Kalman filter.

Once x, y and z are estimated, the estimates of the declination angle, $\hat{\beta}$, and the right ascension angle, $\hat{\alpha}$, are computed as follows

$$\hat{\beta} = \tan^{-1}\left(\frac{\sqrt{\hat{x}^2 + \hat{y}^2}}{\hat{z}}\right) \tag{16.c}$$

$$\hat{\alpha} = \tan^{-1}\left(\frac{\hat{y}}{\hat{x}}\right) \tag{16.d}$$

Using the two-argument inverse-tangent function yields the angles in the correct quadrant.

**V.2 A simple KF for (spin) phase angle determination**

It is evident from Fig. 1 that once the orientation of $\mathbf{Z}_b$ has been determined, its location and the location of **s** in GCI coordinates define the reference for the phase angle $\gamma$. As seen in Fig. 5, each time the sun is acquired by the sun sensor, $\gamma$ is equal to $\vartheta_s$, or $\vartheta_s$ plus multiples of $2\pi$. Therefore, the phase angle, $\gamma$, has to be determined only between sun measurements. This is accomplished by prediction using the estimated spin rate. In order to obtain superior prediction, we use a two state KF in which, during the measurement update stage, we improve the zero sun angle estimate and the spin rate. During the prediction phase we compute the best estimate of the phase angle. The dynamics equation of this filter is

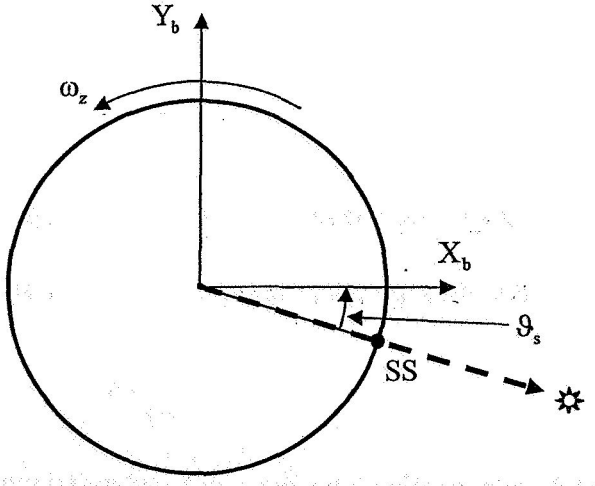


**Fig. 5:** Upper View of a Spinner Cross Section

$$\begin{bmatrix}\dot{\gamma}\\ \dot{\omega}\end{bmatrix} = \begin{bmatrix}0 & 1\\ -1/\tau_\omega & 0\end{bmatrix}\begin{bmatrix}\gamma\\ \omega\end{bmatrix} + \begin{bmatrix}w_\gamma\\ w_\omega\end{bmatrix} \tag{17.a}$$

At a sun crossing we have the following measurement

$$2\pi + \vartheta_s = \begin{bmatrix} 1 & 0 \end{bmatrix} \begin{bmatrix} \gamma \\ \omega \end{bmatrix} + v_\gamma \tag{17.b}$$

The value of $\vartheta_s$ is determined from the measurement $\mathbf{s}_b$. From Fig. 6 it is obvious that

$$\vartheta_s = \tan^{-1}\left(\frac{s_{bx}}{s_{by}}\right) \tag{17.c}$$

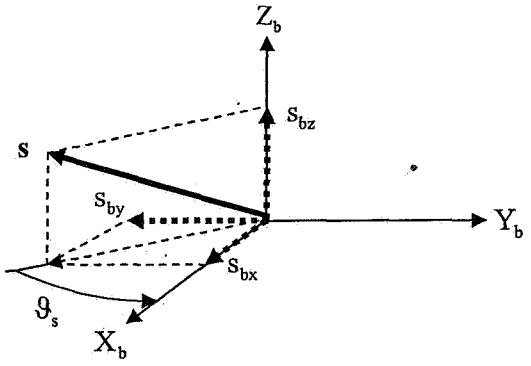


**Fig 6:** The Geometry of $\vartheta_s$

Also at sun crossing we compute

$$\omega_m = \frac{2\pi}{t_n - t_{n-1}} \tag{17.d}$$

where $t_n$ is the present sun crossing time, and $t_{n-1}$ is the previous one. This "measurement" of the spin rate is related to the state vector in Eq. (17.a) by the measurement equation

$$\omega_m = \begin{bmatrix} 0 & 1 \end{bmatrix} \begin{bmatrix} \gamma \\ \omega \end{bmatrix} + v_\omega \tag{17.e}$$

Consequently, at the sun crossing time, one combined measurement update is performed using the measurement equation

$$\begin{bmatrix} 2\pi + \vartheta_s \\ \omega_m \end{bmatrix} = \begin{bmatrix} 1 & 0 \\ 0 & 1 \end{bmatrix} \begin{bmatrix} \gamma \\ \omega \end{bmatrix} + \begin{bmatrix} v_\gamma \\ v_\omega \end{bmatrix} \tag{17.f}$$

Once a measurement update is performed we subtract $2\pi$ from $\gamma$ to start a new cycle modulo $2\pi$.

## VI. Results

ST5 Data were used to evaluate the two filters. The data consisted of the time at which the measurements were taken, $\mathbf{s}_b$, $\mathbf{s}_I$, $\mathbf{m}_b$ and $\mathbf{m}_I$. It should be noted that these time points were the instants in which the sun sensor acquired the sun.

### VI.1 Spin axis filter

We ran the spin axis filter using the following values. The value of $\tau_x$, $\tau_y$, and $\tau_z$ in Eq. (16.b) was 3600 sec. The covariance matrix of the driving force noise was $Q = \text{diag}\{10e-4 \quad 10e-4 \quad 10e-4\}$. The covariance matrix of the measurement noise corresponded to a sun sensor error of 0.1 degree, and that of the magnetometer was 10 milliGauss, thus $R = \text{diag}\{3 \cdot 10e-3 \quad 2.5 \cdot 10e-3\}$. In addition to the filtered, we also computed the unfiltered value of $\mathbf{Z}_b$ in GCI coordinates. This was done using the algorithm presented in Eqs. (14). In Fig. 7 we present the filtered and the unfiltered components of $\mathbf{Z}_b$ in GCI coordinates. The filtered values are plotted using the broken lines and the unfiltered values are designated by the solid lines. Obviously, the initial value of both vectors is identical because both were computed identically. In Fig. 8 we present the angle between the filtered and unfiltered unit vectors.

It turned out that $\mathbf{s}_b$ did not quite correspond to $\mathbf{s}_I$, and, similarly $\mathbf{m}_b$, did not quite correspond to $\mathbf{m}_I$. It was assumed that this stemmed from the fact that the measurements were not ideal. Another indication to this effect was the difference between the $z$ - element of $D_I^{bT}\mathbf{s}_I$ and of $\mathbf{s}_b$, and between the $z$ - element of $D_I^{bT}\mathbf{m}_I$ and of $\mathbf{m}_b$. This was obvious when checking the orthogonality of the matrix $D_I^b$ computed according to Eq. (14.d).

Therefore we tried an additional approach to compute the filtered $\mathbf{Z}_b$ in GCI coordinates. We used Eqs. (14.a – d) to compute $D_I^b$ and then we applied to it Singular Value Decomposition

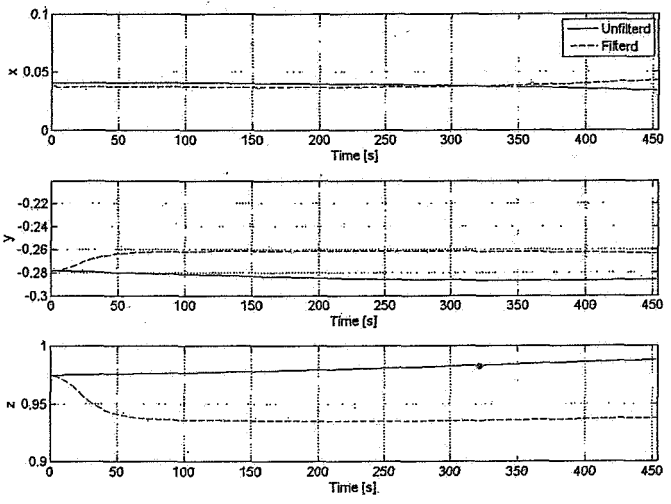


**Fig. 7:** The Filtered and Unfiltered Components of $\mathbf{Z}_b$ in GCI Coordinates.

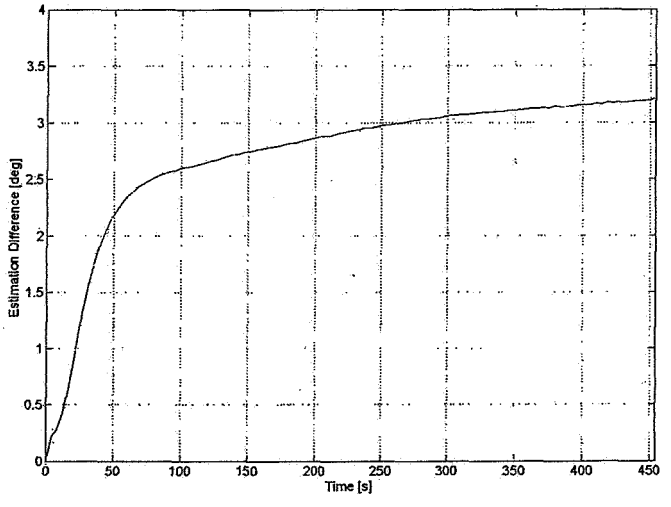


**Fig. 8:** The Angular Difference between the Unfiltered and Filtered Vectors.

in order to obtain $D_{I,ort}^b$, the closest orthogonal matrix to $D_I^b$. Next we used $D_{I,ort}^b$ to transform $\mathbf{s}_I$ and $\mathbf{m}_I$ to $\mathbf{s}_b$ and $\mathbf{m}_b$, respectively, and used these $\mathbf{s}_b$ and $\mathbf{m}_b$ as measured vectors in

body coordinates. The filter was then applied to the latter, and the results were termed refined-filtered components of $\mathbf{Z}_b$. It should be mentioned that the application of the TRIAD algorithm to the data would have also rendered an orthogonal $D_I^b$; however, it would not have been the orthogonal matrix closest to $D_I^b$; moreover, the result of TRIAD depends on which vector of the two, sun or magnetic field vector, is the one used to start the algorithm. We plotted the refined-filtered versus the unfiltered spin axis components in Fig. 9. The angular difference between the two vectors is plotted in Fig. 10.

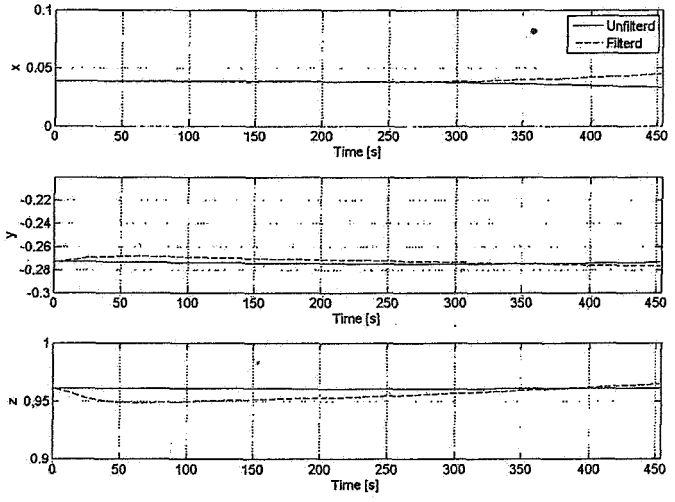


**Fig. 9:** The Refined-Filtered and Unfiltered Components of $\mathbf{Z}_b$ in GCI Coordinates.

### VI.2 Spin (phase) angle filter

The filter described in Section V.2 was applied to the sun sensor timing data. The value of $\tau_\omega$ was 36000 sec. The covariance matrix of the white driving noise was $Q_p = \text{diag}\{10e-4 \quad 10e-4\}$. The initial value of $\vartheta_s$ was computed according to Eq. (17.c), and the initial value of the estimated angular rate was chosen to be zero. As measurements we used the $\mathbf{s}_b$ vectors which were used in the refined-filter. The covariance of the measurement error, $r_s$, was chosen as $3 \cdot 10e-6$. The behavior of the phase angle is described in Fig. 11.

The stars designate the value of the estimated $\vartheta_s$ at the beginning of a new cycle. In order to see the nature of the phase angle, $\gamma$, only the first few cycles are presented. The estimated spin rate is shown in Fig. 12.

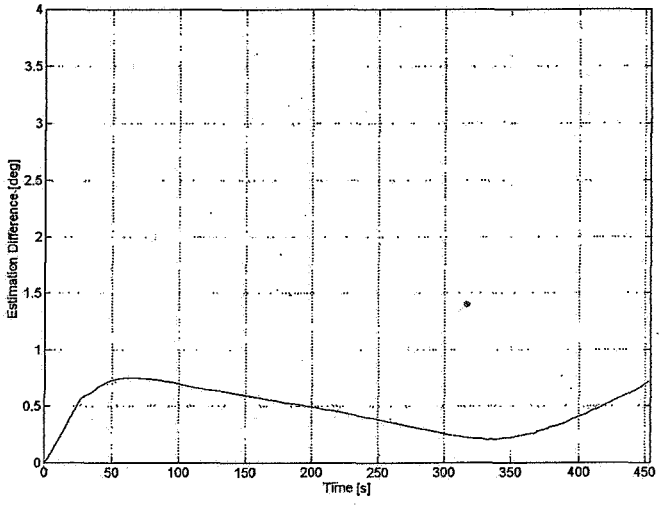


**Fig. 10:** Angular Difference between the Refined-Filtered and the Unfiltered Vectors.

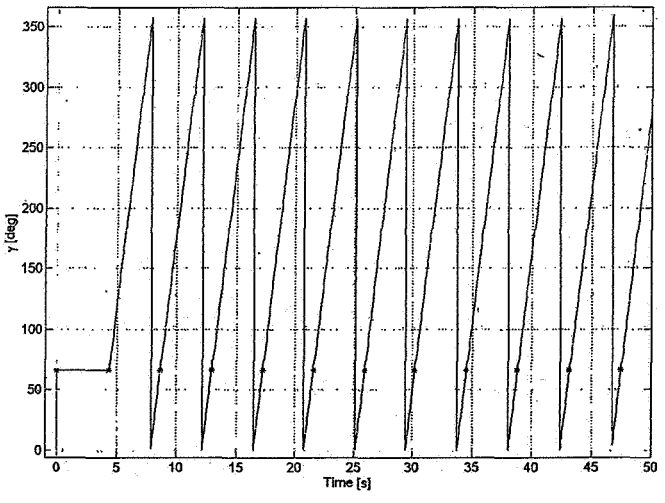


**Fig. 11:** Spin (Phase) Angle Estimate.

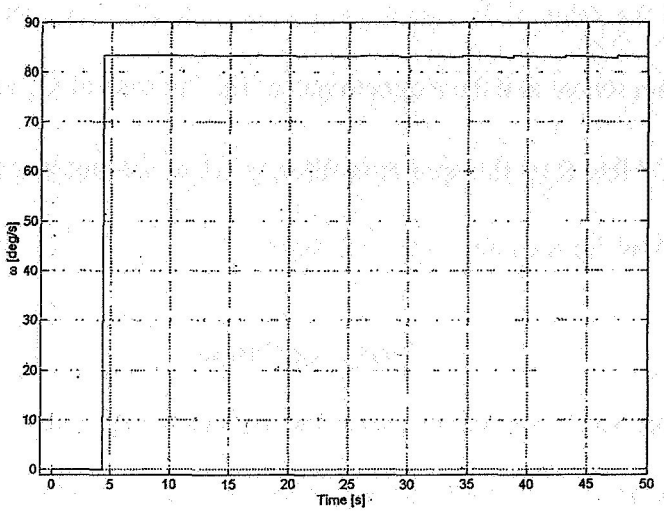


**Fig. 12:** Spin Rate Estimate.

## VII. Discussion

As mentioned earlier, there was a discrepancy between the measured sun and the measured magnetic field vectors in body on one hand, and their corresponding vectors in the GCI coordinates on the other hand. This was obvious when using these vectors to compute the transformation matrix from body to inertial coordinates or vice versa. The discrepancy manifested itself in non-orthogonality of the transformation matrix. We attempted to correct this discrepancy by using the data to find the DCM that corresponds to each set of measurements, compute the orthogonal matrix closest to it, and then use it to transform the inertial data to body data, and treat it as the measured data to which we applied the spin axis filter. It is impossible to tell which plots better describe the orientation of $\mathbf{Z}_b$, because we do not have the reference attitude.

We investigated the sensitivity of the filters. It was found that decreasing the time constants in the dynamics model increased the difference between the filtered and unfiltered components of $\mathbf{Z}_b$. That difference was insensitive to the change in the value of Q of that

model. Note that the value of R was not a design variable but was rather determined by the accuracy of the sun sensor and the magnetometer. The increase of $Q_p$ had very little influence on the estimates. Like R of the spin axis filter, $r_s$ also was not a design variable, but was rather determined by the accuracy of the sun sensor.

## VIII. Conclusions

In this work we presented a new recursive filter to estimate the attitude of a spinning SC. It is based on the separation of the attitude representation into the representation of the spin axis orientation by its components in the GCI system, and the spin (phase) angle about this axis. This approach enables the separation of the filter into two low-order simple filters, one of which estimated the slowly varying components of the spin axis, and the other estimated the phase angle and the spin rate. Even though the spin angle changes fast, its filter is very simple because the spin axis and the spin rate are almost constant. Both filters are independent of the SC dynamics model, which is one of the factors that make the filters so simple. The ambiguity problem is solved using vector calculations, which avoids tedious spherical geometry computations. ST5 satellite data were used to test the filters, and the sensitivity to filter parameter change was examined. Although there were no data to compare the results with, the results indicated that the filters performed well.

## Acknowledgement

We wish to thank Mr. Mark Koifman of the Philadelphia Flight Control Laboratory of the Faculty of Aerospace Engineering of the Technion – Israel Institute of Technology for programming the Kalman filters and running them.

**References**

[1]Wertz, J.R. (ed.), *Spacecraft Attitude Determination and Control*, D. Reidel Publishing Co., Dordrecht, The Netherlands, 1997.

[2]Baker, D.F., "An Extended Kalman Filter for Spinning Spacecraft Attitude Estimation", Proceedings of the Flight Mechanics/Estimation Theory Symposium 1991. NASA Conference Publication 3123. pp. 385-402.

[3]Markley, F.L., Seidewitz, E. and Nicholson, M., "A General Model for Attitude Determination Error Analysis," Proceedings of the Flight Mechanics/Estimation Theory Symposium 1988. NASA Conference Publication 3011. pp. 3-25.

[4]Sedlak, J., "Spinning Spacecraft Attitude Estimation Using Markley Variables: Filter Implementation and Results", Proceedings of the Flight Mechanics Symposium 2005. NASA-Goddard Space Flight Center, Greenbelt, MD 20771, October 18-20, 2005.

[5]Markley, F.L., "New Dynamics Variables for Rotating Spacecraft," AAS-93-330, Proceedings of the International Symposium on Space Flight Dynamics, NASA/GSFC, Greenbelt, MD, Advances in the Astronautical Sciences, Vol. 84, Univelt, San Diego, 1993.

[6]Bar-Itzhack, I.Y., and Harman, R.R., "Pseudolinear and State-Dependent Riccati Equation Filters for Angular Rate Estimation", *AIAA J. of Guidance, Control, and Dynamics*, Vol. 22, No. 5, Sept.-Oct. 1999, pp. 723-725.

[7]Bar-Itzhack, I.Y. and Harman, R.R., "Pseudo-Linear Attitude Determination of Spinning Spacecraft," (in preparation).

[8]Shuster, M.D., "Efficient Algorithm for Spin-Axis Attitude Estimation," *The Journal of the Astronautical Sciences*, Vol. 31, No. 2, April-June 1983, pp. 237-249.

[9]Grubin, C., "Simple Algorithm for Intersecting Two Conical Surfaces," *Journal of Spacecraft and Rockets*, Vol. 14, No. 4, April 1977, pp. 251- 252.

[10]van der Ha, J.C., "Equal-Chord Attitude determination Method of Spinning Spacecraft," *Journal of the Guidance, Control, and Dynamics*, Vol. 28, No. 5, September-October 2005, pp. 997-1105.

[11]Blake, H.D., "A Passive System for Determining the Attitude of a Satellite, "*AIAA Journal*, Vol. 2, No. 7, 1964, pp. 1350, 1351.

[12]Shuster, M.D., and Oh, S.D., "Three-Axis Attitude Determination from Vector Observations," *Journal of Guidance and Control*, Vol. 4, No. 1, 1981, pp. 70 –77.

[13]Singer, R.A., "Estimating Optimal Tracking Filter Performance for Manned Maneuvering Targets," *IEEE Transactions on Aerospace and Electronic Systems*, Vol. AES-6, No.4, July 1970. pp. 473-483.